



Simultaneous detection of mercury and cadmium ions: A colorimetric method in aqueous media

Behzad Pourbadiei^a, Bagher Eftekhari-Sis^b, Azadeh Kordzadeh^c, Ali Pourjavadi^{a,*}

^a Department of Chemistry, Sharif University of Technology, Tehran, 11365-9516, Iran

^b Department of Chemistry, University of Maragheh, Maragheh, 55181-83111, Iran

^c Department of Chemical and Petroleum Engineering, Sharif University of Technology, Tehran, 11365-9516, Iran

ARTICLE INFO

Keywords:

Chemosensor
Mercury detection
pH indicator
Heavy metal ions

ABSTRACT

Hg and Cd are the two most toxic heavy metal ions that could be found in aqueous solutions. In this study, a chemosensor based on 5-(4-((4-nitrophenyl) diazenyl) phenyl)-1,3,4-oxadiazole-2-thiol (DOT) was reported to detect these ions simultaneously. DOT showed high selectivity towards Hg ion by changing the color of the solution from beige to gold-yellow at different concentrations of Hg ion. In comparison, other relevant metals, such as Li^+ , Na^+ , K^+ , Cs^+ , Mg^{2+} , Ca^{2+} , Al^{3+} , Fe^{2+} , Ag^+ , Cu^{2+} , Pb^{2+} , Ni^{2+} , Zn^{2+} , Cr^{3+} , Fe^{3+} , Pb^{4+} , Mn^{2+} , and Cd^{2+} did not affect the color of the DOT solution as the interfering ions. Despite no changes in the color of DOT solution in the presence of Cd ion, a solution containing DOT-Hg complex was changed from gold-yellow to orange by adding Cd ion, providing an approach for detecting Hg and Cd ion simultaneously with UV-Vis and Fluorescent spectroscopy. DOT exhibited a high association constant with a detection limit of 0.05 μM for Hg and Cd ions in an aqueous solution. The results of quantum mechanics (QM) calculations were also consistent with the experimental observations, which indicated that changes in the band gap could explain the various colors of DOT complex with metal ions.

1. Introduction

Water and soil contamination has always been a noticeable matter in environmental studies, leading to the developing and designing heavy metal ions receptors [1–4]. Mercury is a highly toxic metal [5–7] and its compounds are used in various industries and present in wastewaters, which can accumulate in living organisms. Constant exposure to mercury can cause permanent damage to DNA besides disorders in the brain, kidney, lungs, stomatitis, and digestive system [8,9], as well as neurological problems and other severe diseases like acrodynea, Hunter-Russell, Minamata, and even death [10–13]. On the other hand, cadmium is a very toxic metal found on earth and is commonly used in industry, military affairs, agriculture, and metallurgy. Chronic exposure to Cd ion can cause severe health disorders like renal dysfunction, calcium metabolism disorders, and diseases such as pneumonitis, pulmonary edema, emphysema, and even cancer [14–18]. The extent of toxicity for mercury and cadmium brings the necessity of monitoring them in environmental sources and drinking water with high selectivity and sensitivity. Therefore, developing reliable methods for qualitative and quantitative determination of these ions in aqueous media is particularly interesting. Several analytical techniques, including inductively coupled plasma mass spectrometry [19,20], inductively coupled plasma-atomic emission spectrometry [21,22], atomic

* Corresponding author.

E-mail address: purjavad@sharif.edu (A. Pourjavadi).

absorption/emission spectrometry [18,23], atomic fluorescence spectrometry [24–26], high-performance liquid chromatography [27], voltammetry [28], and flame photometry [29] are used for the determination of Hg and Cd ions. Despite their excellent performance, these methods require expensive apparatus, complicated sample preparation, and are time-consuming. Hence, considerable attention has been paid to develop optical fluorescent sensors or colorimetric chemosensors. Although a variety of chemosensors for Hg and Cd ions were developed based on small molecules [30,31], bio-molecules [32,33], polymers [34,35], and nanoparticles [36], most of them rely on fluorescence enhancement (turn-on) or quenching (turn-off) approaches; and it is highly desirable to design novel colorimetric sensors for simple, low-cost, and naked-eye detection of these ions without resort to any spectroscopic equipment. Therefore, the design and synthesis of colorimetric chemosensors for simultaneous detection of Hg and Cd ions are of interest [37–40].

This study reported a selective and sensitive colorimetric and fluorescent chemosensor based on DOT for Hg and Cd ions [41,42]. The UV–Vis and fluorescence spectra determined heavy metal ions with DOT. The outcome of spectroscopies revealed that the prepared sensor can detect even trace amounts of Hg ions with shifting of the UV–Vis spectra. Interestingly, the results suggested that DOT can detect Cd ions in the presence of Hg ions by raising a new absorbance peak at 515 nm, while DOT caused no shift in the UV spectra of Cd ions. To prove the mentioned statement, different molar ratios of Hg and Cd were mixed with DOT and it was obvious that increase in the molar ratio of Cd ions convert the mixture color gradually from yellow to orange; up to the point that the sample included only Cd ions, which no color change and UV–Vis spectra shift was observed. Furthermore, photoluminescence spectroscopy showed “turn-on” state in case of the presence of Hg ions, which confirm that DOT could be used as a simultaneous detector for both Hg and Cd ions. Investigations illustrated that the pH of the solution can make differences on the observed color, which acidic and basic environment resulted in yellowish and blue, respectively.

Also, quantum mechanical (QM) calculations were performed to calculate molecular orbitals and reveal the molecular mechanisms which could not be assessed experimentally. To this aim, the band gap energies of DOT were calculated in the presence of various ions [43], which could explain the color changes in solutions. Moreover, by mimicking the expected structure of complexes, the binding energies between distinct ions and DOT were studied to find the most stable structure to verify the stoichiometry of the formation process of complexes. The results were in complete agreement with the observations of earlier tests, which suggested that this method could provide a great chemosensor in aqueous media.

2. Experimental

2.1. Materials and methods

Carbon disulfide (CS₂), ethyl benzoate, hydrazine monohydrate, sodium nitrite (NaNO₂), 4-nitroaniline, NaOH and HCl (36 %), ethanol, deionized water, and all the metal ions came in as acetate salts. All materials were purchased from Sigma-Aldrich without any further purification. Solvents were used as received from commercial suppliers. ¹H-NMR 500 MHz Bruker, FT-IR PerkinElmer 781 spectrometer, UV–Vis PerkinElmer Lambda 25 spectrophotometer, and JASCO-FP-750, Rev. 1.00 fluorometer.

2.2. Synthesis of 5-(4-((4-nitrophenyl) diazenyl) phenyl)-1,3,4-oxadiazole-2-thiol (DOT)

Firstly, to obtain benzoic hydrazide, an excess amount of hydrazine (0.64 g, 20 mmol) was added to ethyl benzoate (2.25 g, 15 mmol) in ethanol solution and refluxed for 6 h. Then 0.1 g of NaOH in 2 mL of water and 0.3 mL of CS₂ were added to a benzoic hydrazide solution (0.182 g, 1.34 mmol) in 6–7 mL of EtOH, and the resulting mixture was refluxed for 4 h. After completion of the reaction, EtOH was evaporated under reduced pressure, and then 4 mL of water was added and acidified with a diluted HCl to pH = 5. The 5-Phenyl-1,3,4-oxadiazol-2-thiol, was collected as a white precipitate by filtration (Yield: 76 %, m.p. 211–213 °C). Then, 5-Phenyl-1,3,4-oxadiazol-2-thiol (0.356 g, 2 mmol) was dissolved in a solution of KOH (0.6 g in 6 mL water) in an ice bath and was slowly added

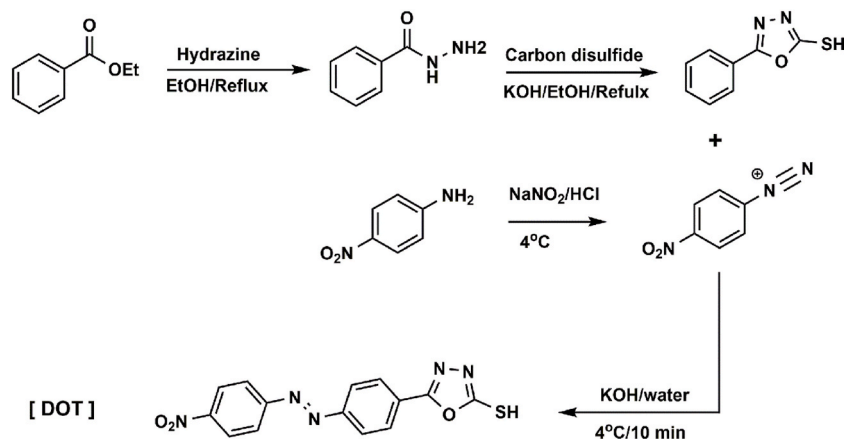


Fig. 1. Preparation of 5-(4-((4-nitrophenyl) diazenyl) phenyl)-1,3,4-oxadiazole-2-thiol (receptor DOT).

to a cooled solution of sodium nitrite (0.138 g, 2 mmol), and for diazo coupling reaction, 4-nitroaniline (0.304 g, 2.2 mmol) in 15 mL of HCl solution (10 %) was poured to the mixture (Fig. 1). The final solution was stirred for 10 min in an ice bath and filtered for removal of byproducts, then the filtrate was left to dry and a yellow precipitate was obtained (Isolated Yield: 50 %, m.p. 223–224.5 °C), FT-IR (KBr) $\nu = 3269$ (C–H), 2401 (S–H), 1596 (C=C), 1517, 1334 (NO₂), 1404 (N=N), 1254 (C–O) cm⁻¹; ¹H NMR (500 MHz, DMSO-*d*₆) $\delta = 13.54$ (s, 1H, SH), 8.32 (m, 4H, CH_{Ar}), 7.84 (d, *J* = 7.6 Hz, 2H, CH_{Ar}), 7.32 (d, *J* = 7.6 Hz, 2H, CH_{Ar}) (Fig. S1). Also, the CHNS data of DOT are reported in Table S1.

3. Results and discussion

3.1. UV–Vis spectroscopy and quantum mechanics studies

To explore the sensing behavior of DOT toward metal ions, UV–Vis spectroscopy was carried out on free DOT, which showed a peak centered at 415 nm, and also in the presence of various metal ions, including Li⁺, Na⁺, K⁺, Cs⁺, Mg²⁺, Ca²⁺, Al³⁺, Ag⁺, Cu²⁺, Pb²⁺, Ni²⁺, Cd²⁺, Zn²⁺, Cr³⁺, Pb⁴⁺, Hg²⁺, and Mn²⁺ in a DMSO/water (1:1) solution; the concentration of metal ions and DOT was 20 μ M and 1 μ M, respectively. After adding an aqueous solution of Hg ion to the solution of DOT, the absorption band was red shifted to 460 nm, and the beige color of DOT was changed to a gold-yellow color. Studies showed that other relevant metal ions did not cause any changes in the absorption spectra of DOT (Fig. 2a). A titration was performed to study the limit of detection of DOT solution towards the concentration of Hg ions. The obtained results in Fig. S2 indicated that the limit of detection of Hg ion equals 0.05 μ M. Upon adding the Hg ion to the DOT solution, the initial absorption at 415 nm was red shifted, and a new peak appeared at 460 nm due to the intramolecular charge transfer between DOT and Hg ions. A simultaneous increase in the absorbance at 460 nm and a decrease in the absorbance at 415 nm were observed in the UV–Vis spectra. The isosbestic point verifies the equilibrium between DOT and Hg ions, confirming the free DOT changes to the DOT-Hg complex. A linear response of the A/A₀ as a function of Hg ion concentration at 460 nm was observed in the range of 0.5–20 μ M (Fig. 2b). The kinetic studies of the complex formation of DOT-Hg were investigated. As shown in Fig. S3 almost 70% of the complex formation is done in 1 min. It confirms the fast complex formation which is due to strong binding constant between DOT and Hg which equals 1.94×10^8 M⁻¹ based on obtained results in Fig. S4.

The first-principal QM tools were used to reveal the intermolecular interactions of DOT, and the used methods were explained in SI. The highest occupied molecular orbital (HOMO) and lowest unoccupied molecular orbital (LUMO) for DOT were calculated and represented in Fig. 2c. It is known that a HOMO is a nucleophile with a higher eigenvalue than LUMO as an electrophile. Fig. 2c indicates that the DOT molecule has a band gap equal to 2.9840 eV. As shown in Fig. S5, the bonding energy between mercury and DOT was calculated for different complexes to find the most stable DOT-Hg complex. The distance of Hg ion from the nearest atoms in these energy-minimized complexes is also displayed. According to the results, Hg ion bonded to sulfur as a nucleophile site has the highest binding energy, equal to 75.6144 kJ/mol. The comparison between Fig. 2c and d showed that the DOT molecules bonded to mercury

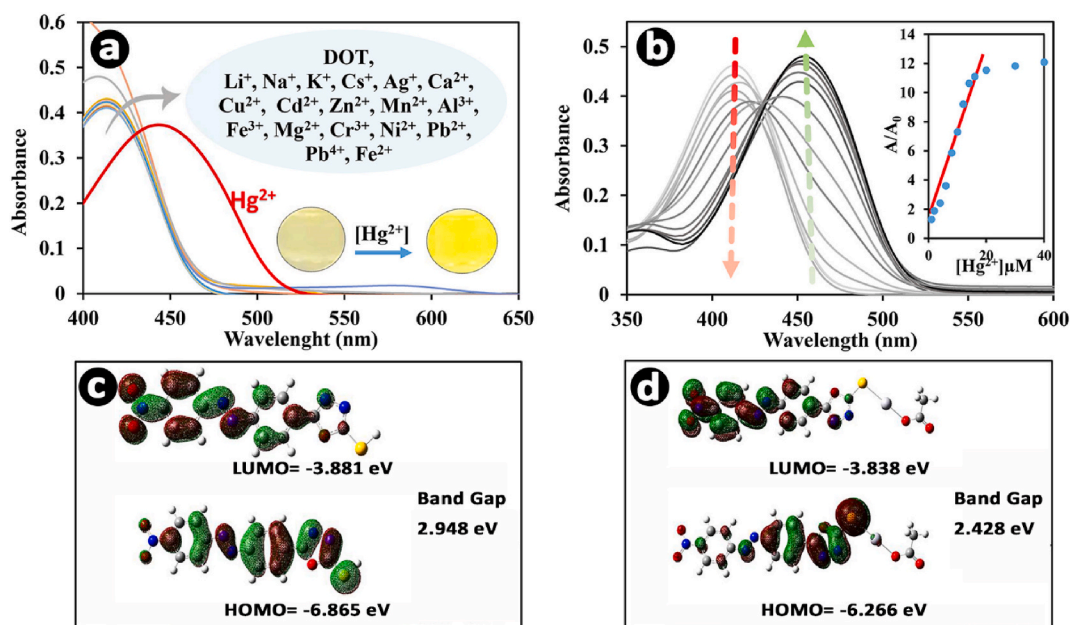


Fig. 2. UV–Vis spectra and the color changes of DOT upon addition of various metal ions (a), UV–Vis spectra of DOT by titration with Hg ion (0.05–40 μ M) and A/A₀ as a function of Hg ion concentration at 460 nm (b), the HOMO and LUMO of DOT (c), and DOT-Hg (d). The positive and negative surfaces are presented with red and green colors, respectively. The carbon, nitrogen, hydrogen, oxygen, and sulfur atoms are shown with cyan, blue, white, red, and yellow spheres, respectively. (For interpretation of the references to color in this figure legend, the reader is referred to the Web version of this article.)

have a lower band gap (2.428 eV) than free DOT. The Fukui indices of DOT are reported in Table S2, and also the graphical results for electrophilic and nucleophilic attacks of DOT are depicted in Fig. S6. The represented results demonstrate that sulfur possessed a large f^- function value (0.176) and could donate electrons to an electrophile, while the NO_2 group is an electron acceptor due to a considerable value of f^+ function. Finally, it can be concluded that the nucleophile and electrophile sites of DOT agree with the corresponding HOMO and LUMO, respectively.

3.2. Job's plot: DOT-Hg stoichiometry

Job's method was used to study the stoichiometry of bindings between DOT and Hg ions. The measurements were performed by UV-Vis absorbance at wavelength of 460 nm of the DOT-Hg solutions varying the molar ratio of Hg ion from 0 to 1; the total concentrations of Hg ion and DOT were kept constant at 20 μM . Fig. 3a shows a 1:1 stoichiometry of the binding mode of DOT with Hg ion. Further studies of the optimized geometries of different DOT-Hg complexes obtained from QM computations are represented in Fig. 3b. To understand the DOT-Hg complex stoichiometries, the total energy of the complexes was calculated for the two most likely stoichiometries of 1:1 and 2:1 (DOT: Hg). It is evident that the total energy of DOT decreases from -35886 eV to -57149 eV in the presence of Hg ion bonded to DOT. While the 2:1 stoichiometry has an energy value equal to -29684 eV, indicating that 1:1 stoichiometry is more stable as obtained in Job's plot.

3.3. Investigations of interfering metal ions

Two competitive metal ions titrations were conducted to investigate the utilization of DOT for selective detection of Hg ions in the presence of other metal ions. Firstly, a solution of DOT (1 μM) and Hg ion (20 μM) was titrated with an excess amount (2-fold) of other metal ions. The addition of Al^{3+} , Fe^{3+} , and Cr^{3+} caused a complete color change of DOT-Hg complex, resembling the color of free DOT, and shifted the absorbance peak from 460 nm to around 415 nm. Also, based on theoretical investigations, three valence ions (Al^{3+} , Fe^{3+} , and Cr^{3+}) were placed near the NO_2 group because the Cd ion, had the maximum binding energy (166.8243 kJ/mol) near to NO_2 group of DOT-Hg in theoretical calculations (Fig. S7). The results indicated that the band gap energies in the presence of these ions (Al^{3+} , Fe^{3+} , and Cr^{3+}) are the same as free DOT, which causes a blue shift to 415 nm (Figs. S8 and S9). Interestingly, by adding the Cd ion, the absorbance peak of DOT-Hg shifted from 460 nm to 515 nm. In the case of other metal ions such as Li^+ , Na^+ , K^+ , Cs^+ , Mg^{2+} , Ca^{2+} , Ag^+ , Pb^{2+} , Ni^{2+} , Zn^{2+} , Fe^{2+} , Cu^{2+} , Mn^{2+} , Co^{2+} , Ce^{3+} , and Pb^{4+} , there is not any change neither in the UV-Vis spectrum nor in the color of the DOT-Hg solution (Fig. 4a and b). It is essential to investigate the impact of adding Hg ions to the solution of DOT complexed with other metal ions. Therefore, in the second experiment, a solution of DOT (1 μM) and each metal ion (40 μM) was titrated with Hg ion solution (20 μM). The interaction of DOT with Hg ions in the presence of other metals was strong enough to cause a color change of the solution to gold-yellow with an absorbance peak at 460 nm, except for Cd ions which caused a peak to emerge at 515 nm (Fig. 4c and d).

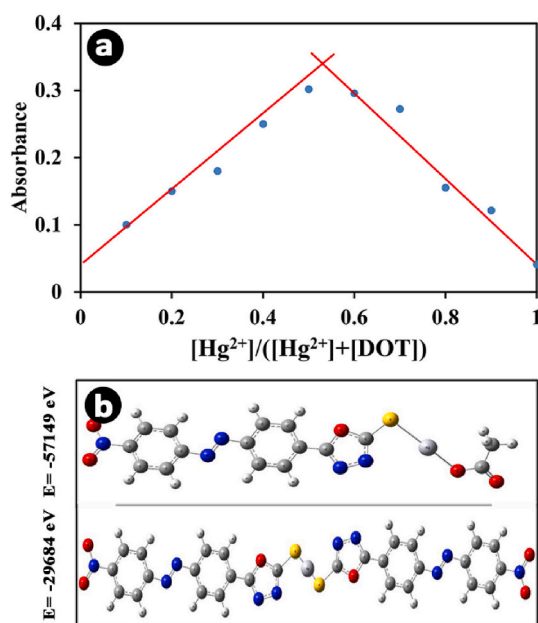


Fig. 3. Job's plot to determine binding stoichiometry between DOT and Hg ion (a), the optimized structure of DOT complex with their total energies (b).

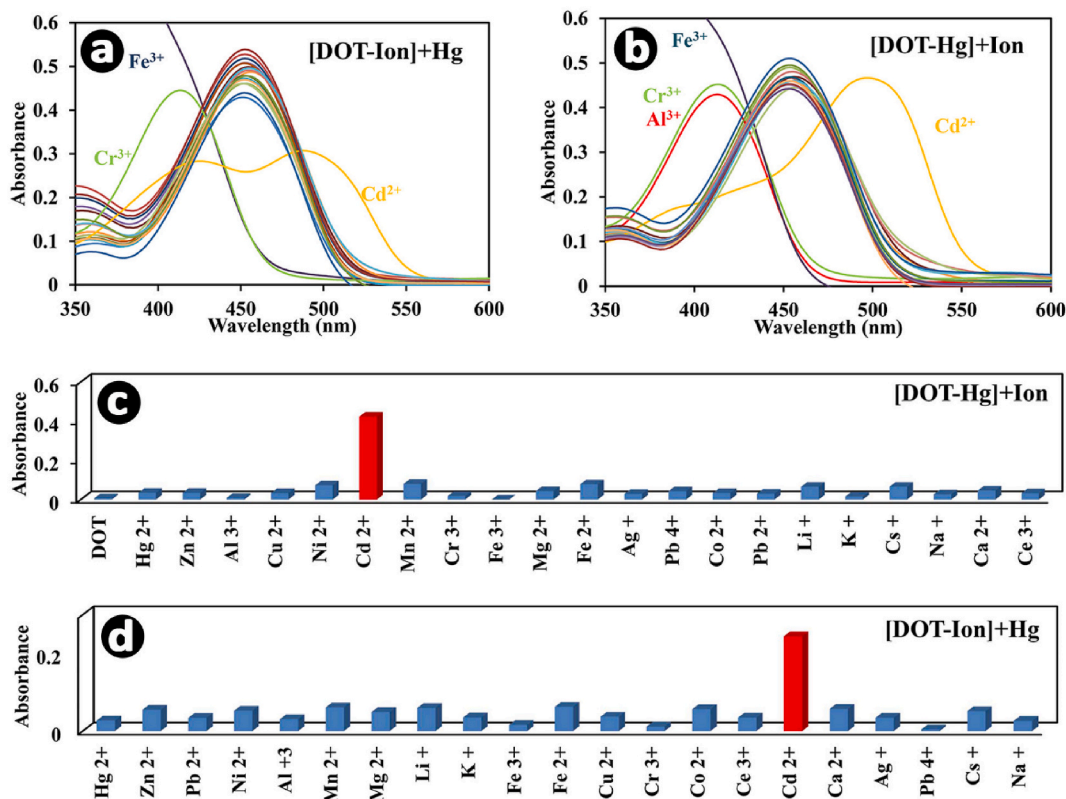


Fig. 4. The effect of adding Hg ion on the UV–Vis absorbance of DOT complexed with competitive metal ions (a), the effect of adding competitive metal ions on the UV–Vis absorbance of DOT–Hg (b). Also, the absorption peaks at 515 nm are demonstrated in (c) and (d), respectively.

3.4. Simultaneously detection of Hg and Cd ions

3.4.1. UV–Vis spectroscopy investigations

As mentioned, the DOT–Cd has the same absorbance peak as free DOT at 415 nm. However, it would change in the presence of the Hg ion. This phenomenon was intriguing to design an experiment to determine the simultaneous detection of Cd and Hg ions. To this aim, as shown in both cases ($\text{Cd}^{2+} + [\text{DOT-Hg}]$) and ($\text{Hg}^{2+} + [\text{DOT-Cd}]$), a band appeared at 515 nm, and the color of the solution changed from gold-yellow to orange.

Then, the measurement of Hg and Cd ions with DOT was studied by UV–Vis absorbance titration by two different methods. First, a solution of DOT (1 μM) and Hg ion (20 μM) was titrated with a solution of Cd ion ranging from 0 to 40 μM in water. The intensity of the DOT–Hg complex peak at 460 nm decreased gradually, and a new band at 515 nm appeared associated with DOT–Hg–Cd complex, which was enhanced by increasing the Cd ion concentration (Fig. S10). An excellent linear response of A_{515}/A_{460} as a function of Cd ion concentration in the range of 1–40 μM was observed, which could be used to measure the concentration of Cd ion in the presence of DOT–Hg complex (Fig. 5a and S11). In the second experiment, a solution of DOT (1 μM) and Cd ion (20 μM) was titrated by a solution of Hg ion ranging from 0 to 40 μM in water. The solution of DOT–Cd complex showed the same absorbance of free DOT at 415 nm, which red shifted to 515 nm, associated with the DOT–Cd–Hg complex in low concentration of Hg ion (0.05–12 μM). Surprisingly, in a high concentration of Hg ion (15–40 μM), the band at 515 nm blue shifted to 460 nm gradually, related to the DOT–Hg complex, which indicates the overcoming of DOT–Hg to DOT–Cd–Hg complex in a competitive interaction. The A_{460}/A_{515} plot exhibited good linearity as a function of Hg ion concentrations ranging from 15 to 40 μM (Fig. 5b and S10).

In addition, the ratio at both wavelengths, A_{515}/A_{460} , exhibited good linearity as a function of the mole ratio of Hg ions in the range of 0.2–0.8 (Fig. 6a). The color change of the solution is obvious in Fig. 6b, which could be determined by the naked eye for the detection of Hg and Cd ions simultaneously. To determine the bonding site of Cd on DOT–Hg complex, different DOT–Hg–Cd complexes were investigated with QM computations. The optimized geometries are represented in Fig. S7. The distance of the Cd ion from the nearest atoms in these energy-minimized complexes is also displayed. On the other hand, when the Cd ion forms a complex with DOT–Hg, the band gap decreases to 1.994 eV (Fig. S8a), which is lower than DOT. To confirm the effect of Cd on DOT, the cadmium ions were placed at 6 probable places, and the energy level was calculated, as it is shown in Fig. S12. The energy level of DOT in presence of Cd ion is similar to DOT which equals -28519.7231 eV.

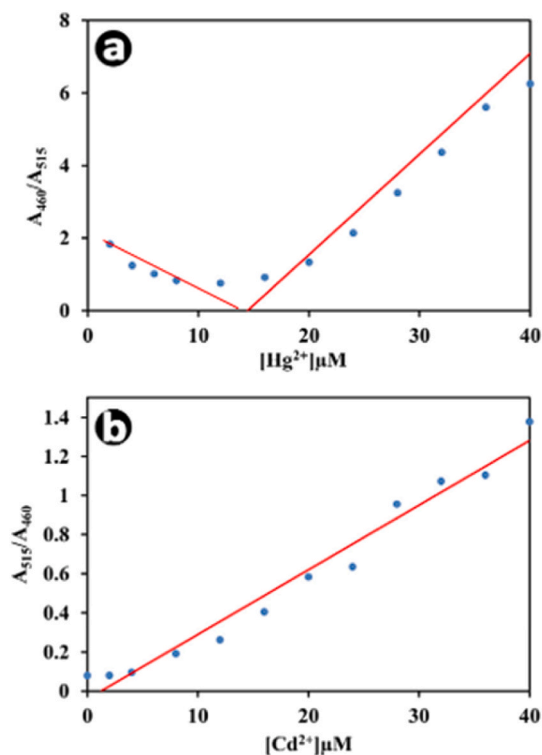


Fig. 5. A460/A515 ratio of the solution of DOT-Hg-Cd as a function of Hg ion concentration (a), and A515/A460 ratio of the solution of DOT-Hg-Cd as a function of Cd ion concentration (b).

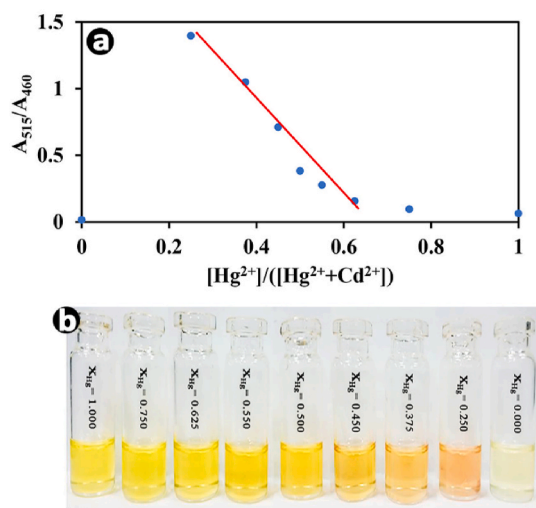


Fig. 6. A515/A460 ratio of the solution of DOT-Hg-Cd as a function of Hg ion mole ratio(a), and the color change of the solutions by varying Hg ion mole ratio (b). (For interpretation of the references to color in this figure legend, the reader is referred to the Web version of this article.)

3.4.2. Photoluminescence spectroscopy investigations

The fluorescence spectroscopy of DOT was also studied upon adding various metal ions. The fluorescence emission was observed for the DOT-Hg complex because its band gap is lower than for free DOT. The addition of Hg ions resulted in fluorescence emission at 550 nm. In contrast, other relevant ions did not cause any changes in the fluorescence spectra of DOT (Fig. 7a). Afterward, the sensitivity of DOT towards Hg ion concentration was investigated by titration of DOT (Fig. 7b). The normalized intensity $[(I_{\min}-I)/(I_{\min}-I_{\max})]$ was plotted against $\log [Hg^{2+}]$, which exhibited an excellent linearity behavior (Fig. 7c). According to computational studies, the band gap energies of DOT-Hg and DOT-Hg-Cd complexes (2.428 eV and 1.994 eV respectively) are lower than the energy of

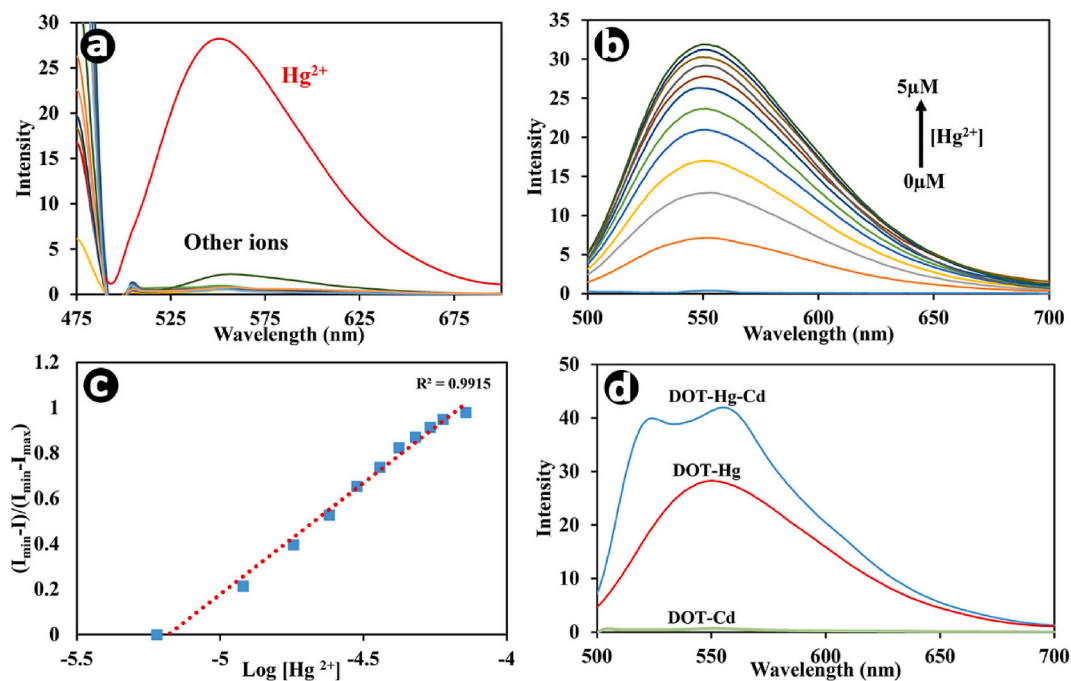


Fig. 7. Fluorescence spectra of DOT upon addition of different metal ions excited with 475 nm light (a), fluorescence spectra of DOT by titration with Hg ion in the range 0–5 μM (b), and normalized emission intensity $[(I_{\text{min}}-I)/(I_{\text{min}}-I_{\text{max}})]$ as a function of Hg ion concentration (c), fluorescence spectra of DOT-Hg, DOT-Cd and DOT-Hg-Cd (d).

475 nm exciting light (2.610 eV) which resulted in the emission of fluorescence light. In contrast, the band gap energies of complexes of DOT with other ions are more than 2.610 eV, which causes no fluorescence emission (Fig. 7d).

3.5. The effect of pH on DOT

The effect of pH on the UV–Vis absorption spectra of DOT was investigated by acid-base titration, exhibiting an absorption band at 415 nm at pH ranges from 0 to 7. The increase of the pH caused a vivid red shift, resulting in the appearance of a broad band at 580 nm at pH equal to 8 and more (Fig. 8a). Computational investigations on the charge of DOT molecules at different pH suggested that the charge is -1 at pH = 8, which verifies the experimental results of λ_{max} shifting (Fig. 8b). Moreover, the comparison between the electron distribution of the HOMO in both neutral (Fig. 2c) and negative (Fig. 8c) forms of DOT indicates that the resonance length of the negative form is shorter than that for the neutral one. Also, the negative form of DOT has a band gap energy equal to 1.719 eV, which is lower than that for the neutral form (2.948 eV). These differences cause the absorption of all the wavelengths in visible light except red, by the negative form observed in violet. While the neutral form could only absorb the wavelengths in the range of violet lights based on its band gap energy; therefore, it would be seen as yellow (Table S3, Fig. 8d).

4. Conclusions

In summary, a chemosensor for simultaneous detection of Hg and Cd ions was developed based on the receptor DOT. A color change was observed in the synthesized receptor upon adding Hg ions, from beige to gold-yellow, whereas other relevant ions did not respond accordingly. Interestingly, the color of DOT-Hg complex solution changes to orange by adding Cd ion, providing a methodology for naked eye detection of Cd ion in the presence of Hg ions. In addition, UV–Vis spectroscopy showed a linear correlation between the intensity of absorbance peaks and the concentrations of Hg and Cd ions were approved. The selectivity and sensitivity of DOT to Hg ions were also studied using fluorescent measurements, in which the normalized emission intensity exhibited linearity toward $\log [\text{Hg}^{2+}]$. The QM calculations demonstrated that the color change of the DOT is due to the change in its electronic structure. By formation of DOT-Hg complex, the band gap decreased from 2.948 eV to 2.428 eV, and as a result, fluorescence emission was observed for the DOT-Hg complex. Finally, the computational and experimental studies revealed that the prepared receptor is a highly selective chemosensor in aqueous media for heavy metals, including Hg and Cd ions, and an excellent pH indicator.

CRedit authorship contribution statement

Behzad Pourbadiei: Investigation, Methodology, Validation, Writing – original draft, Writing – review & editing. **Bagher**

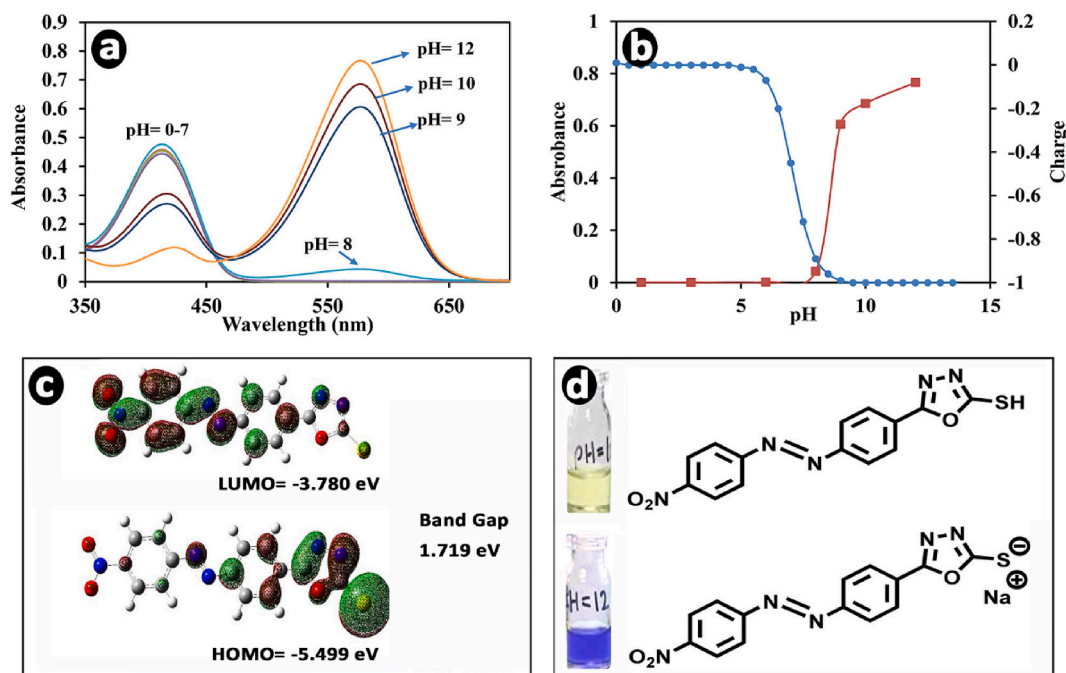


Fig. 8. UV-Vis spectra in various pH (a), the coincidence of λ_{max} shifting and changing of the charge based on computational studies during titration (b), band gap energy of HOMO and LUMO of negative charged DOT (c), the color of DOT solution in acidic and basic media (d). (For interpretation of the references to color in this figure legend, the reader is referred to the Web version of this article.)

Eftekhari-Sis: Methodology, Writing – original draft. **Azadeh Kordzadeh:** Data curation, Methodology, Software. **Ali Pourjavadi:** Funding acquisition, Methodology, Project administration, Supervision, Writing – review & editing.

Declaration of competing interest

The authors declare the following financial interests/personal relationships which may be considered as potential competing interests: Ali Pourjavadi reports was provided by Sharif University of Technology. Ali Pourjavadi reports a relationship with Sharif University of Technology that includes: board membership.

Appendix A. Supplementary data

Supplementary data to this article can be found online at <https://doi.org/10.1016/j.heliyon.2023.e21674>.

References

- [1] H. Na Kim, W. Xiu Ren, J. Seung Kim, J. Yoon, Fluorescent and colorimetric sensors for detection of lead, cadmium, and mercury ions, *Chem. Soc. Rev.* 41 (2012) 3210–3244, <https://doi.org/10.1039/c1cs15245a>.
- [2] H. Obaid, L. Ma, S.E. Nader, M.H. Hashimi, S. Sharifi, H. Kakar, J. Ni, C. Ni, Heavy metal contamination status of water, agricultural soil, and plant in the semiarid region of kandahar, Afghanistan, *ACS Earth Space Chem.* (2023), <https://doi.org/10.1021/acsearthspacechem.3c00095>.
- [3] Mds. Parvez, S. Nawshin, S. Sultana, Mds. Hossain, MdH. Rashid Khan, Mda. Habib, Z.T. Nijhum, R. Khan, Evaluation of heavy metal contamination in soil samples around rampal, Bangladesh, *ACS Omega* 8 (2023) 15990–15999, <https://doi.org/10.1021/acsomega.2c07681>.
- [4] R.B. González-González, E.A. Flores-Contreras, E. González-González, N.E. Torres Castillo, R. Parra-Saldívar, H.M.N. Iqbal, Biosensor constructs for the monitoring of persistent emerging pollutants in environmental matrices, *Ind. Eng. Chem. Res.* 62 (2023) 4503–4520, <https://doi.org/10.1021/acs.iecr.2c00421>.
- [5] P. Thirupathi, P. Saritha, K.H. Lee, Ratiometric fluorescence chemosensor based on tyrosine derivatives for monitoring mercury ions in aqueous solutions, *Org. Biomol. Chem.* 12 (2014) 7100–7109, <https://doi.org/10.1039/c4ob01044b>.
- [6] J. Ni, H. Hu, L. Wu, Fabrication of calcium peroxide into amphiphilic nest-like attapulgite/SiO₂ as a seed coating nanocomposite of wheat that confers resistance to multiple environmental stresses, *ACS Agricultural Science & Technology* 2 (2022) 1300–1310, <https://doi.org/10.1021/acscagritech.2c00255>.
- [7] X. Liu, X. Gong, D. Zhou, Q. Jiang, Y. Liang, R. Ye, S. Zhang, Y. Wang, X. Tang, F. Li, J. Yi, Plant defensin-dissimilar thionin *OsThi9* alleviates cadmium toxicity in rice plants and reduces cadmium accumulation in rice grains, *J. Agric. Food Chem.* 71 (2023) 8367–8380, <https://doi.org/10.1021/acs.jafc.3c01032>.
- [8] P.B. Tchounwou, W.K. Ayensu, N. Ninashvili, D. Sutton, Environmental exposure to mercury and its toxicopathologic implications for public health, *Environ. Toxicol.* 18 (2003) 149–175, <https://doi.org/10.1002/tox.10116>.
- [9] T. Li, Y. Song, X. Yuan, J. Li, J. Ji, X. Fu, Q. Zhang, S. Guo, Incorporating bioaccessibility into human health risk assessment of heavy metals in rice (*Oryza sativa* L.): a probabilistic-based analysis, *J. Agric. Food Chem.* 66 (2018) 5683–5690, <https://doi.org/10.1021/acs.jafc.8b01525>.

- [10] Y.H. Huang, X.Y. Jin, Y.Y. Zhao, H. Cong, Z. Tao, A fluorescence-enhanced chemosensor based on multifarene[2,2] and its recognition of metal cations, *Org. Biomol. Chem.* 16 (2018) 5343–5349, <https://doi.org/10.1039/c8ob01315b>.
- [11] J. Wang, X. Feng, C.W.N. Anderson, Y. Xing, L. Shang, Remediation of mercury contaminated sites - a review, *J. Hazard Mater.* (2012) 221–222, <https://doi.org/10.1016/j.jhazmat.2012.04.035>, 1–18.
- [12] T. Syversen, P. Kaur, The toxicology of mercury and its compounds, *J. Trace Elem. Med. Biol.* 26 (2012) 215–226, <https://doi.org/10.1016/j.jtemb.2012.02.004>.
- [13] M. Uchimiya, D. Bannon, H. Nakanishi, M.B. McBride, M.A. Williams, T. Yoshihara, Chemical speciation, plant uptake, and toxicity of heavy metals in agricultural soils, *J. Agric. Food Chem.* 68 (2020) 12856–12869, <https://doi.org/10.1021/acs.jafc.0c00183>.
- [14] B.P. Joshi, C.R. Lohani, K.H. Lee, A highly sensitive and selective detection of Hg(II) in 100% aqueous solution with fluorescent labeled dimerized Cys residues, *Org. Biomol. Chem.* 8 (2010) 3220–3226, <https://doi.org/10.1039/b925744f>.
- [15] M. Waisberg, P. Joseph, B. Hale, D. Beyersmann, Molecular and cellular mechanisms of cadmium carcinogenesis, *Toxicology* 192 (2003) 95–117, [https://doi.org/10.1016/S0300-483X\(03\)00305-6](https://doi.org/10.1016/S0300-483X(03)00305-6).
- [16] R.K. Zalups, S. Ahmad, Molecular handling of cadmium in transporting epithelia, *Toxicol. Appl. Pharmacol.* 186 (2003) 163–188, [https://doi.org/10.1016/S0041-008X\(02\)00021-2](https://doi.org/10.1016/S0041-008X(02)00021-2).
- [17] T. Zeng, R. Zhang, Y. Chen, W. Guo, J. Wang, Z. Cai, In situ localization of lipids on mouse kidney tissues with acute cadmium toxicity using atmospheric pressure-MALDI mass spectrometry imaging, *Talanta* 245 (2022), 123466, <https://doi.org/10.1016/j.talanta.2022.123466>.
- [18] Q. Ba, J. Zhou, J. Li, S. Cheng, X. Zhang, H. Wang, Mutagenic characteristics of six heavy metals in *Escherichia coli*: the commonality and specificity, *Environ. Sci. Technol.* 56 (2022) 13867–13877, <https://doi.org/10.1021/acs.est.2c04785>.
- [19] B.M.W. Fong, S.S. Tak, J.S.K. Lee, S. Tam, Determination of mercury in whole blood and urine by inductively coupled plasma mass spectrometry, *J. Anal. Toxicol.* 31 (2007) 281–287, <https://doi.org/10.1093/jat/31.5.281>.
- [20] L. Xia, B. Hu, Z. Jiang, Y. Wu, Y. Liang, Single-drop microextraction combined with low-temperature electrothermal vaporization ICPMS for the determination of trace Be, Co, Pd, and Cd in biological samples, *Anal. Chem.* 76 (2004) 2910–2915, <https://doi.org/10.1021/ac035437e>.
- [21] X. Chai, X. Chang, Z. Hu, Q. He, Z. Tu, Z. Li, Solid phase extraction of trace Hg(II) on silica gel modified with 2-(2-oxoethyl)hydrazine carbothioamide and determination by ICP-AES, *Talanta* 82 (2010) 1791–1796, <https://doi.org/10.1016/j.talanta.2010.07.076>.
- [22] S. Satarug, J.R. Baker, S. Urbenjapol, M. Haswell-Elkins, P.E.B. Reilly, D.J. Williams, M.R. Moore, A global perspective on cadmium pollution and toxicity in non-occupationally exposed population, *Toxicol. Lett.* 137 (2003) 65–83, [https://doi.org/10.1016/S0378-4274\(02\)00381-8](https://doi.org/10.1016/S0378-4274(02)00381-8).
- [23] J. Wang, S.M. Shaheen, C.W.N. Anderson, Y. Xing, S. Liu, J. Xia, X. Feng, J. Rinklebe, Nanoactivated carbon reduces mercury mobility and uptake by *Oryza sativa L*: mechanistic investigation using spectroscopic and microscopic techniques, *Environ. Sci. Technol.* 54 (2020) 2698–2706, <https://doi.org/10.1021/acs.est.9b05685>.
- [24] L.N. Neupane, P.K. Mehta, J.U. Kwon, S.H. Park, K.H. Lee, Selective red-emission detection for mercuric ions in aqueous solution and cells using a fluorescent probe based on an unnatural peptide receptor, *Org. Biomol. Chem.* 17 (2019) 3590–3598, <https://doi.org/10.1039/C8OB03224F>.
- [25] H. Li, Z. Xu, N. Sun, Porphyrin-infiltrated SiO₂ inverse opal photonic crystal as fluorescence sensor for selective detection of trace mercury ion, *Opt. Mater.* 122 (2021), 111696, <https://doi.org/10.1016/j.optmat.2021.111696>.
- [26] F. Matloubi Moghaddam, B. Aghamiri, Facile one-pot, multi-component reaction to synthesize spirooxindole-annulated thiopyran derivatives under environmentally benovolent conditions, *Heliyon* 8 (2022), e10666, <https://doi.org/10.1016/j.heliyon.2022.e10666>.
- [27] S. Ichinoki, N. Kitahata, Y. Fujii, Selective determination of mercury(II) ion in water by solvent extraction followed by reversed-phase HPLC, *J. Liq. Chromatogr. Relat. Technol.* 27 (2004) 1785–1798, <https://doi.org/10.1081/JLC-120037371>.
- [28] A. Pourjavadi, M. Doroudian, A. Ahadpour, B. Pourbadiei, Preparation of flexible and free-standing graphene-based current collector via a new and facile self-assembly approach: leading to a high performance porous graphene/polyaniline supercapacitor, *Energy* 152 (2018) 178–189, <https://doi.org/10.1016/j.energy.2018.03.138>.
- [29] F.S. Rojas, C.B. Oieda, J.M.C. Pavón, Dispersive liquid-liquid microextraction combined with flame atomic absorption spectrometry for determination of cadmium in environmental, water and food samples, *Anal. Methods* 3 (2011) 1652–1655, <https://doi.org/10.1039/c1ay05188a>.
- [30] M.H. Yang, P. Thirupathi, K.H. Lee, Selective and sensitive ratiometric detection of Hg(II) ions using a simple amino acid based sensor, *Org. Lett.* 13 (2011) 5028–5031, <https://doi.org/10.1021/ol201683t>.
- [31] W. Wang, Q. Wen, Y. Zhang, X. Fei, Y. Li, Q. Yang, X. Xu, Simple naphthalimide-based fluorescent sensor for highly sensitive and selective detection of Cd²⁺ and Cu²⁺ in aqueous solution and living cells, *Dalton Trans.* 42 (2013) 1827–1833, <https://doi.org/10.1039/c2dt32279j>.
- [32] L. Deng, Z. Zhou, J. Li, T. Li, S. Dong, Fluorescent silver nanoclusters in hybridized DNA duplexes for the turn-on detection of Hg²⁺ ions, *Chem. Commun.* 47 (2011) 11065–11067, <https://doi.org/10.1039/c1cc14012d>.
- [33] Y. Li, L. Li, X. Pu, G. Ma, E. Wang, J. Kong, Z. Liu, Y. Liu, Synthesis of a ratiometric fluorescent peptide sensor for the highly selective detection of Cd²⁺, *Bioorg Med Chem Lett* 22 (2012) 4014–4017, <https://doi.org/10.1016/j.bmcl.2012.04.088>.
- [34] E.S. Childress, C.A. Roberts, D.Y. Sherwood, C.L.M. Leguyader, E.J. Harbron, Ratiometric fluorescence detection of mercury ions in water by conjugated polymer nanoparticles, *Anal. Chem.* 84 (2012) 1235–1239, <https://doi.org/10.1021/ac300022y>.
- [35] M.F. Philips, A.I. Gopalan, K.P. Lee, Development of a novel cyano group containing electrochemically deposited polymer film for ultrasensitive simultaneous detection of trace level cadmium and lead, *J. Hazard Mater.* (2012) 237–238, <https://doi.org/10.1016/j.jhazmat.2012.07.069>, 46–54.
- [36] X.-Y. Liu, Z.-L. Zhao, T.-T. Hao, X. Li, A simply visual and rapidly colorimetric detection of Hg²⁺ in cosmetics based on gold nanoparticles modified by sulfadiazine, *Opt. Mater.* 137 (2023), 113622, <https://doi.org/10.1016/j.optmat.2023.113622>.
- [37] R. Manjumeena, D. Durairabu, T. Rajamuthuramalingam, R. Venkatesan, P.T. Kalaichelvan, Highly responsive glutathione functionalized green AuNP probe for precise colorimetric detection of Cd²⁺ contamination in the environment, *RSC Adv.* 5 (2015) 69124–69133, <https://doi.org/10.1039/c5ra12427a>.
- [38] H. Chen, W. Hu, C.M. Li, Colorimetric detection of mercury(II) based on 2,2'-bipyridyl induced quasi-linear aggregation of gold nanoparticles, *Sensor. Actuator. B Chem.* 215 (2015) 421–427, <https://doi.org/10.1016/j.snb.2015.03.083>.
- [39] N. Chen, J. Chen, J.H. Yang, L.Y. Bai, Y.P. Zhang, Colorimetric detection of cadmium ions using DL-mercaptosuccinic acid-modified gold nanoparticles, *J. Nanosci. Nanotechnol.* 16 (2016) 840–843, <https://doi.org/10.1166/jnn.2016.11618>.
- [40] Y. Qi, Y. Li, T. Nan, H. Li, J. Tang, S. Liu, Y. Wang, A novel fluorescent probe with large Stokes shift for the detection of Ag⁺ and Hg²⁺, *Opt. Mater.* 123 (2022), 111929, <https://doi.org/10.1016/j.optmat.2021.111929>.
- [41] A. Pourjavadi, S. Rahemipoor, M. Kohestanian, Synthesis and characterization of multi stimuli-responsive block copolymer-silica hybrid nanocomposite with core-shell structure via RAFT polymerization, *Compos. Sci. Technol.* 188 (2020), 107951, <https://doi.org/10.1016/j.compscitech.2019.107951>.
- [42] B. Eftekhari-Sis, M. Zirak, A. Akbari, Arylglyoxals in synthesis of heterocyclic compounds, *Chem. Rev.* 113 (2013) 2958–3043, <https://doi.org/10.1021/cr300176g>.
- [43] S. Şahin, M.O. Caglayan, Z. Üstündağ, A review on nanostructure-based mercury (II) detection and monitoring focusing on aptamer and oligonucleotide biosensors, *Talanta* 220 (2020), 121437, <https://doi.org/10.1016/J.TALANTA.2020.121437>.